

A Measurement of CP Asymmetry in $b \rightarrow s\gamma$ using a Sum of Exclusive Final States

B. Aubert,¹ M. Bona,¹ Y. Karyotakis,¹ J. P. Lees,¹ V. Poireau,¹ X. Prudent,¹ V. Tisserand,¹ A. Zghiche,¹ J. Garra Tico,² E. Grauges,² L. Lopez,³ A. Palano,³ M. Pappagallo,³ G. Eigen,⁴ B. Stugu,⁴ L. Sun,⁴ G. S. Abrams,⁵ M. Battaglia,⁵ D. N. Brown,⁵ J. Button-Shafer,⁵ R. N. Cahn,⁵ R. G. Jacobsen,⁵ J. A. Kadyk,⁵ L. T. Kerth,⁵ Yu. G. Kolomensky,⁵ G. Kukartsev,⁵ G. Lynch,⁵ I. L. Osipenkov,⁵ M. T. Ronan,^{5,*} K. Tackmann,⁵ T. Tanabe,⁵ W. A. Wenzel,⁵ C. M. Hawkes,⁶ N. Soni,⁶ A. T. Watson,⁶ H. Koch,⁷ T. Schroeder,⁷ D. Walker,⁸ D. J. Asgeirsson,⁹ T. Cuhadar-Donszelmann,⁹ B. G. Fulsom,⁹ C. Hearty,⁹ T. S. Mattison,⁹ J. A. McKenna,⁹ M. Barrett,¹⁰ A. Khan,¹⁰ M. Saleem,¹⁰ L. Teodorescu,¹⁰ V. E. Blinov,¹¹ A. D. Bukin,¹¹ A. R. Buzykaev,¹¹ V. P. Druzhinin,¹¹ V. B. Golubev,¹¹ A. P. Onuchin,¹¹ S. I. Serednyakov,¹¹ Yu. I. Skovpen,¹¹ E. P. Solodov,¹¹ K. Yu. Todyshev,¹¹ M. Bondioli,¹² S. Curry,¹² I. Eschrich,¹² D. Kirkby,¹² A. J. Lankford,¹² P. Lund,¹² M. Mandelkern,¹² E. C. Martin,¹² D. P. Stoker,¹² S. Abachi,¹³ C. Buchanan,¹³ J. W. Gary,¹⁴ F. Liu,¹⁴ O. Long,¹⁴ B. C. Shen,^{14,*} G. M. Vitug,¹⁴ Z. Yasin,¹⁴ L. Zhang,¹⁴ H. P. Paar,¹⁵ S. Rahatlou,¹⁵ V. Sharma,¹⁵ C. Campagnari,¹⁶ T. M. Hong,¹⁶ D. Kovalskyi,¹⁶ M. A. Mazur,¹⁶ J. D. Richman,¹⁶ T. W. Beck,¹⁷ A. M. Eisner,¹⁷ C. J. Flacco,¹⁷ C. A. Heusch,¹⁷ J. Kroseberg,¹⁷ W. S. Lockman,¹⁷ T. Schalk,¹⁷ B. A. Schumm,¹⁷ A. Seiden,¹⁷ M. G. Wilson,¹⁷ L. O. Winstrom,¹⁷ E. Chen,¹⁸ C. H. Cheng,¹⁸ D. A. Doll,¹⁸ B. Echenard,¹⁸ F. Fang,¹⁸ D. G. Hitlin,¹⁸ I. Narsky,¹⁸ T. Piatenko,¹⁸ F. C. Porter,¹⁸ R. Andreassen,¹⁹ G. Mancinelli,¹⁹ B. T. Meadows,¹⁹ K. Mishra,¹⁹ M. D. Sokoloff,¹⁹ F. Blanc,²⁰ P. C. Bloom,²⁰ W. T. Ford,²⁰ J. F. Hirschauer,²⁰ A. Kreisel,²⁰ M. Nagel,²⁰ U. Nauenberg,²⁰ A. Olivas,²⁰ J. G. Smith,²⁰ K. A. Ulmer,²⁰ S. R. Wagner,²⁰ R. Ayad,^{21,†} A. M. Gabareen,²¹ A. Soffer,^{21,‡} W. H. Toki,²¹ R. J. Wilson,²¹ D. D. Altenburg,²² E. Feltresi,²² A. Hauke,²² H. Jasper,²² M. Karbach,²² J. Merkel,²² A. Petzold,²² B. Spaan,²² K. Wacker,²² V. Klose,²³ M. J. Kobel,²³ H. M. Lacker,²³ W. F. Mader,²³ R. Nogowski,²³ J. Schubert,²³ K. R. Schubert,²³ R. Schwierz,²³ J. E. Sundermann,²³ A. Volk,²³ D. Bernard,²⁴ G. R. Bonneau,²⁴ E. Latour,²⁴ Ch. Thiebaut,²⁴ M. Verderi,²⁴ P. J. Clark,²⁵ W. Gradl,²⁵ S. Playfer,²⁵ A. I. Robertson,²⁵ J. E. Watson,²⁵ M. Andreotti,²⁶ D. Bettoni,²⁶ C. Bozzi,²⁶ R. Calabrese,²⁶ A. Cecchi,²⁶ G. Cibinetto,²⁶ P. Franchini,²⁶ E. Luppi,²⁶ M. Negrini,²⁶ A. Petrella,²⁶ L. Piemontese,²⁶ E. Prencipe,²⁶ V. Santoro,²⁶ F. Anulli,²⁷ R. Baldini-Ferroli,²⁷ A. Calcaterra,²⁷ R. de Sangro,²⁷ G. Finocchiaro,²⁷ S. Pacetti,²⁷ P. Patteri,²⁷ I. M. Peruzzi,^{27,§} M. Piccolo,²⁷ M. Rama,²⁷ A. Zallo,²⁷ A. Buzzo,²⁸ R. Contri,²⁸ M. Lo Vetere,²⁸ M. M. Macri,²⁸ M. R. Monge,²⁸ S. Passaggio,²⁸ C. Patrignani,²⁸ E. Robutti,²⁸ A. Santroni,²⁸ S. Tosi,²⁸ K. S. Chaisanguanthum,²⁹ M. Morii,²⁹ R. S. Dubitzky,³⁰ J. Marks,³⁰ S. Schenk,³⁰ U. Uwer,³⁰ D. J. Bard,³¹ P. D. Dauncey,³¹ J. A. Nash,³¹ W. Panduro Vazquez,³¹ M. Tibbetts,³¹ P. K. Behera,³² X. Chai,³² M. J. Charles,³² U. Mallik,³² J. Cochran,³³ H. B. Crawley,³³ L. Dong,³³ V. Egyes,³³ W. T. Meyer,³³ S. Prell,³³ E. I. Rosenberg,³³ A. E. Rubin,³³ Y. Y. Gao,³⁴ A. V. Gritsan,³⁴ Z. J. Guo,³⁴ C. K. Lae,³⁴ A. G. Denig,³⁵ M. Fritsch,³⁵ G. Schott,³⁵ N. Arnaud,³⁶ J. Béquilleux,³⁶ A. D’Orazio,³⁶ M. Davier,³⁶ J. Firmino da Costa,³⁶ G. Grosdidier,³⁶ A. Höcker,³⁶ V. Lepeltier,³⁶ F. Le Diberder,³⁶ A. M. Lutz,³⁶ S. Pruvot,³⁶ P. Roudeau,³⁶ M. H. Schune,³⁶ J. Serrano,³⁶ V. Sordini,³⁶ A. Stocchi,³⁶ W. F. Wang,³⁶ G. Wormser,³⁶ D. J. Lange,³⁷ D. M. Wright,³⁷ I. Bingham,³⁸ J. P. Burke,³⁸ C. A. Chavez,³⁸ J. R. Fry,³⁸ E. Gabathuler,³⁸ R. Gamet,³⁸ D. E. Hutchcroft,³⁸ D. J. Payne,³⁸ C. Touramanis,³⁸ A. J. Bevan,³⁹ K. A. George,³⁹ F. Di Lodovico,³⁹ R. Sacco,³⁹ M. Sigamani,³⁹ G. Cowan,⁴⁰ H. U. Flaecher,⁴⁰ D. A. Hopkins,⁴⁰ S. Paramesvaran,⁴⁰ F. Salvatore,⁴⁰ A. C. Wren,⁴⁰ D. N. Brown,⁴¹ C. L. Davis,⁴¹ K. E. Alwyn,⁴² N. R. Barlow,⁴² R. J. Barlow,⁴² Y. M. Chia,⁴² C. L. Edgar,⁴² G. D. Lafferty,⁴² T. J. West,⁴² J. I. Yi,⁴² J. Anderson,⁴³ C. Chen,⁴³ A. Jawahery,⁴³ D. A. Roberts,⁴³ G. Simi,⁴³ J. M. Tuggle,⁴³ C. Dallapiccola,⁴⁴ S. S. Hertzbach,⁴⁴ X. Li,⁴⁴ E. Salvati,⁴⁴ S. Saremi,⁴⁴ R. Cowan,⁴⁵ D. Dujmic,⁴⁵ P. H. Fisher,⁴⁵ K. Koeneke,⁴⁵ G. Sciolla,⁴⁵ M. Spitznagel,⁴⁵ F. Taylor,⁴⁵ R. K. Yamamoto,⁴⁵ M. Zhao,⁴⁵ S. E. McLachlin,^{46,*} P. M. Patel,⁴⁶ S. H. Robertson,⁴⁶ A. Lazzaro,⁴⁷ V. Lombardo,⁴⁷ F. Palombo,⁴⁷ J. M. Bauer,⁴⁸ L. Cremaldi,⁴⁸ V. Eschenburg,⁴⁸ R. Godang,⁴⁸ R. Kroeger,⁴⁸ D. A. Sanders,⁴⁸ D. J. Summers,⁴⁸ H. W. Zhao,⁴⁸ S. Brunet,⁴⁹ D. Côté,⁴⁹ M. Simard,⁴⁹ P. Taras,⁴⁹ F. B. Viaud,⁴⁹ H. Nicholson,⁵⁰ G. De Nardo,⁵¹ L. Lista,⁵¹ D. Monorchio,⁵¹ C. Sciacca,⁵¹ M. A. Baak,⁵² G. Raven,⁵² H. L. Snoek,⁵² C. P. Jessop,⁵³ K. J. Knoepfel,⁵³ J. M. LoSecco,⁵³ G. Benelli,⁵⁴ L. A. Corwin,⁵⁴ K. Honscheid,⁵⁴ H. Kagan,⁵⁴ R. Kass,⁵⁴ J. P. Morris,⁵⁴ A. M. Rahimi,⁵⁴ J. J. Regensburger,⁵⁴ S. J. Sekula,⁵⁴ Q. K. Wong,⁵⁴ N. L. Blount,⁵⁵ J. Brau,⁵⁵ R. Frey,⁵⁵ O. Igonkina,⁵⁵ J. A. Kolb,⁵⁵ M. Lu,⁵⁵ R. Rahmat,⁵⁵ N. B. Sinev,⁵⁵ D. Strom,⁵⁵ J. Strube,⁵⁵ E. Torrence,⁵⁵ G. Castelli,⁵⁶ N. Gagliardi,⁵⁶ A. Gaz,⁵⁶ M. Margoni,⁵⁶ M. Morandin,⁵⁶ M. Posocco,⁵⁶ M. Rotondo,⁵⁶ F. Simonetto,⁵⁶ R. Stroili,⁵⁶ C. Voci,⁵⁶ P. del Amo Sanchez,⁵⁷ E. Ben-Haim,⁵⁷ H. Briand,⁵⁷ G. Calderini,⁵⁷

J. Chauveau,⁵⁷ P. David,⁵⁷ L. Del Buono,⁵⁷ O. Hamon,⁵⁷ Ph. Leruste,⁵⁷ J. Malclès,⁵⁷ J. Ocariz,⁵⁷ A. Perez,⁵⁷
J. Prendki,⁵⁷ L. Gladney,⁵⁸ M. Biasini,⁵⁹ R. Covarelli,⁵⁹ E. Manoni,⁵⁹ C. Angelini,⁶⁰ G. Batignani,⁶⁰ S. Bettarini,⁶⁰
M. Carpinelli,⁶⁰, ¶ A. Cervelli,⁶⁰ F. Forti,⁶⁰ M. A. Giorgi,⁶⁰ A. Lusiani,⁶⁰ G. Marchiori,⁶⁰ M. Morganti,⁶⁰
N. Neri,⁶⁰ E. Paoloni,⁶⁰ G. Rizzo,⁶⁰ J. J. Walsh,⁶⁰ J. Biesiada,⁶¹ Y. P. Lau,⁶¹ D. Lopes Pegna,⁶¹ C. Lu,⁶¹
J. Olsen,⁶¹ A. J. S. Smith,⁶¹ A. V. Telnov,⁶¹ E. Baracchini,⁶² G. Cavoto,⁶² D. del Re,⁶² E. Di Marco,⁶²
R. Faccini,⁶² F. Ferrarotto,⁶² F. Ferroni,⁶² M. Gaspero,⁶² P. D. Jackson,⁶² M. A. Mazzoni,⁶² S. Morganti,⁶²
G. Piredda,⁶² F. Polci,⁶² F. Renga,⁶² C. Voena,⁶² M. Ebert,⁶³ T. Hartmann,⁶³ H. Schröder,⁶³ R. Waldi,⁶³
T. Adye,⁶⁴ B. Franek,⁶⁴ E. O. Olaiya,⁶⁴ W. Roethel,⁶⁴ F. F. Wilson,⁶⁴ S. Emery,⁶⁵ M. Escalier,⁶⁵
A. Gaidot,⁶⁵ S. F. Ganzhur,⁶⁵ G. Hamel de Monchenault,⁶⁵ W. Kozanecki,⁶⁵ G. Vasseur,⁶⁵ Ch. Yéche,⁶⁵
M. Zito,⁶⁵ X. R. Chen,⁶⁶ H. Liu,⁶⁶ W. Park,⁶⁶ M. V. Purohit,⁶⁶ R. M. White,⁶⁶ J. R. Wilson,⁶⁶ M. T. Allen,⁶⁷
D. Aston,⁶⁷ R. Bartoldus,⁶⁷ P. Bechtle,⁶⁷ J. F. Benitez,⁶⁷ R. Cenci,⁶⁷ J. P. Coleman,⁶⁷ M. R. Convery,⁶⁷
J. C. Dingfelder,⁶⁷ J. Dorfan,⁶⁷ G. P. Dubois-Felsmann,⁶⁷ W. Dunwoodie,⁶⁷ R. C. Field,⁶⁷ T. Glanzman,⁶⁷
S. J. Gowdy,⁶⁷ M. T. Graham,⁶⁷ P. Grenier,⁶⁷ C. Hast,⁶⁷ W. R. Innes,⁶⁷ J. Kaminski,⁶⁷ M. H. Kelsey,⁶⁷ H. Kim,⁶⁷
P. Kim,⁶⁷ M. L. Kocian,⁶⁷ D. W. G. S. Leith,⁶⁷ S. Li,⁶⁷ B. Lindquist,⁶⁷ S. Luitz,⁶⁷ V. Luth,⁶⁷ H. L. Lynch,⁶⁷
D. B. MacFarlane,⁶⁷ H. Marsiske,⁶⁷ R. Messner,⁶⁷ D. R. Muller,⁶⁷ H. Neal,⁶⁷ S. Nelson,⁶⁷ C. P. O'Grady,⁶⁷
I. Ofte,⁶⁷ A. Perazzo,⁶⁷ M. Perl,⁶⁷ B. N. Ratcliff,⁶⁷ A. Roodman,⁶⁷ A. A. Salnikov,⁶⁷ R. H. Schindler,⁶⁷
J. Schwiening,⁶⁷ A. Snyder,⁶⁷ D. Su,⁶⁷ M. K. Sullivan,⁶⁷ K. Suzuki,⁶⁷ S. K. Swain,⁶⁷ J. M. Thompson,⁶⁷
J. Va'vra,⁶⁷ A. P. Wagner,⁶⁷ M. Weaver,⁶⁷ W. J. Wisniewski,⁶⁷ M. Wittgen,⁶⁷ D. H. Wright,⁶⁷ H. W. Wulsin,⁶⁷
A. K. Yarritu,⁶⁷ K. Yi,⁶⁷ C. C. Young,⁶⁷ V. Ziegler,⁶⁷ P. R. Burchat,⁶⁸ A. J. Edwards,⁶⁸ S. A. Majewski,⁶⁸
T. S. Miyashita,⁶⁸ B. A. Petersen,⁶⁸ L. Wilden,⁶⁸ S. Ahmed,⁶⁹ M. S. Alam,⁶⁹ R. Bula,⁶⁹ J. A. Ernst,⁶⁹ B. Pan,⁶⁹
M. A. Saeed,⁶⁹ S. B. Zain,⁶⁹ S. M. Spanier,⁷⁰ B. J. Wogsland,⁷⁰ R. Eckmann,⁷¹ J. L. Ritchie,⁷¹ A. M. Ruland,⁷¹
C. J. Schilling,⁷¹ R. F. Schwitters,⁷¹ J. M. Izen,⁷² X. C. Lou,⁷² S. Ye,⁷² F. Bianchi,⁷³ D. Gamba,⁷³
M. Pelliccioni,⁷³ M. Bomben,⁷⁴ L. Bosisio,⁷⁴ C. Cartaro,⁷⁴ F. Cossutti,⁷⁴ G. Della Ricca,⁷⁴ L. Lanceri,⁷⁴
L. Vitale,⁷⁴ V. Azzolini,⁷⁵ N. Lopez-March,⁷⁵ F. Martinez-Vidal,⁷⁵ D. A. Milanes,⁷⁵ A. Oyanguren,⁷⁵ J. Albert,⁷⁶
Sw. Banerjee,⁷⁶ B. Bhuyan,⁷⁶ K. Hamano,⁷⁶ R. Kowalewski,⁷⁶ I. M. Nugent,⁷⁶ J. M. Roney,⁷⁶ R. J. Sobie,⁷⁶
T. J. Gershon,⁷⁷ P. F. Harrison,⁷⁷ J. Ilic,⁷⁷ T. E. Latham,⁷⁷ G. B. Mohanty,⁷⁷ H. R. Band,⁷⁸ X. Chen,⁷⁸
S. Dasu,⁷⁸ K. T. Flood,⁷⁸ P. E. Kutter,⁷⁸ Y. Pan,⁷⁸ M. Pierini,⁷⁸ R. Prepost,⁷⁸ C. O. Vuosalo,⁷⁸ and S. L. Wu⁷⁸

(The BABAR Collaboration)

¹Laboratoire de Physique des Particules, IN2P3/CNRS et Université de Savoie, F-74941 Annecy-Le-Vieux, France

²Universitat de Barcelona, Facultat de Fisica, Departament ECM, E-08028 Barcelona, Spain

³Università di Bari, Dipartimento di Fisica and INFN, I-70126 Bari, Italy

⁴University of Bergen, Institute of Physics, N-5007 Bergen, Norway

⁵Lawrence Berkeley National Laboratory and University of California, Berkeley, California 94720, USA

⁶University of Birmingham, Birmingham, B15 2TT, United Kingdom

⁷Ruhr Universität Bochum, Institut für Experimentalphysik 1, D-44780 Bochum, Germany

⁸University of Bristol, Bristol BS8 1TL, United Kingdom

⁹University of British Columbia, Vancouver, British Columbia, Canada V6T 1Z1

¹⁰Brunel University, Uxbridge, Middlesex UB8 3PH, United Kingdom

¹¹Budker Institute of Nuclear Physics, Novosibirsk 630090, Russia

¹²University of California at Irvine, Irvine, California 92697, USA

¹³University of California at Los Angeles, Los Angeles, California 90024, USA

¹⁴University of California at Riverside, Riverside, California 92521, USA

¹⁵University of California at San Diego, La Jolla, California 92093, USA

¹⁶University of California at Santa Barbara, Santa Barbara, California 93106, USA

¹⁷University of California at Santa Cruz, Institute for Particle Physics, Santa Cruz, California 95064, USA

¹⁸California Institute of Technology, Pasadena, California 91125, USA

¹⁹University of Cincinnati, Cincinnati, Ohio 45221, USA

²⁰University of Colorado, Boulder, Colorado 80309, USA

²¹Colorado State University, Fort Collins, Colorado 80523, USA

²²Universität Dortmund, Institut für Physik, D-44221 Dortmund, Germany

²³Technische Universität Dresden, Institut für Kern- und Teilchenphysik, D-01062 Dresden, Germany

²⁴Laboratoire Leprince-Ringuet, CNRS/IN2P3, Ecole Polytechnique, F-91128 Palaiseau, France

²⁵University of Edinburgh, Edinburgh EH9 3JZ, United Kingdom

²⁶Università di Ferrara, Dipartimento di Fisica and INFN, I-44100 Ferrara, Italy

²⁷Laboratori Nazionali di Frascati dell'INFN, I-00044 Frascati, Italy

²⁸Università di Genova, Dipartimento di Fisica and INFN, I-16146 Genova, Italy

²⁹Harvard University, Cambridge, Massachusetts 02138, USA

³⁰Universität Heidelberg, Philosophischen Institut, Philosophenweg 12, D-69120 Heidelberg, Germany

- ³¹Imperial College London, London, SW7 2AZ, United Kingdom
³²University of Iowa, Iowa City, Iowa 52242, USA
³³Iowa State University, Ames, Iowa 50011-3160, USA
³⁴Johns Hopkins University, Baltimore, Maryland 21218, USA
³⁵Universität Karlsruhe, Institut für Experimentelle Kernphysik, D-76021 Karlsruhe, Germany
³⁶Laboratoire de l'Accélérateur Linéaire, IN2P3/CNRS et Université Paris-Sud 11,
Centre Scientifique d'Orsay, B. P. 34, F-91898 ORSAY Cedex, France
³⁷Lawrence Livermore National Laboratory, Livermore, California 94550, USA
³⁸University of Liverpool, Liverpool L69 7ZE, United Kingdom
³⁹Queen Mary, University of London, E1 4NS, United Kingdom
⁴⁰University of London, Royal Holloway and Bedford New College, Egham, Surrey TW20 0EX, United Kingdom
⁴¹University of Louisville, Louisville, Kentucky 40292, USA
⁴²University of Manchester, Manchester M13 9PL, United Kingdom
⁴³University of Maryland, College Park, Maryland 20742, USA
⁴⁴University of Massachusetts, Amherst, Massachusetts 01003, USA
⁴⁵Massachusetts Institute of Technology, Laboratory for Nuclear Science, Cambridge, Massachusetts 02139, USA
⁴⁶McGill University, Montréal, Québec, Canada H3A 2T8
⁴⁷Università di Milano, Dipartimento di Fisica and INFN, I-20133 Milano, Italy
⁴⁸University of Mississippi, University, Mississippi 38677, USA
⁴⁹Université de Montréal, Physique des Particules, Montréal, Québec, Canada H3C 3J7
⁵⁰Mount Holyoke College, South Hadley, Massachusetts 01075, USA
⁵¹Università di Napoli Federico II, Dipartimento di Scienze Fisiche and INFN, I-80126, Napoli, Italy
⁵²NIKHEF, National Institute for Nuclear Physics and High Energy Physics, NL-1009 DB Amsterdam, The Netherlands
⁵³University of Notre Dame, Notre Dame, Indiana 46556, USA
⁵⁴Ohio State University, Columbus, Ohio 43210, USA
⁵⁵University of Oregon, Eugene, Oregon 97403, USA
⁵⁶Università di Padova, Dipartimento di Fisica and INFN, I-35131 Padova, Italy
⁵⁷Laboratoire de Physique Nucléaire et de Hautes Energies,
IN2P3/CNRS, Université Pierre et Marie Curie-Paris6,
Université Denis Diderot-Paris7, F-75252 Paris, France
⁵⁸University of Pennsylvania, Philadelphia, Pennsylvania 19104, USA
⁵⁹Università di Perugia, Dipartimento di Fisica and INFN, I-06100 Perugia, Italy
⁶⁰Università di Pisa, Dipartimento di Fisica, Scuola Normale Superiore and INFN, I-56127 Pisa, Italy
⁶¹Princeton University, Princeton, New Jersey 08544, USA
⁶²Università di Roma La Sapienza, Dipartimento di Fisica and INFN, I-00185 Roma, Italy
⁶³Universität Rostock, D-18051 Rostock, Germany
⁶⁴Rutherford Appleton Laboratory, Chilton, Didcot, Oxon, OX11 0QX, United Kingdom
⁶⁵DSM/Dapnia, CEA/Saclay, F-91191 Gif-sur-Yvette, France
⁶⁶University of South Carolina, Columbia, South Carolina 29208, USA
⁶⁷Stanford Linear Accelerator Center, Stanford, California 94309, USA
⁶⁸Stanford University, Stanford, California 94305-4060, USA
⁶⁹State University of New York, Albany, New York 12222, USA
⁷⁰University of Tennessee, Knoxville, Tennessee 37996, USA
⁷¹University of Texas at Austin, Austin, Texas 78712, USA
⁷²University of Texas at Dallas, Richardson, Texas 75083, USA
⁷³Università di Torino, Dipartimento di Fisica Sperimentale and INFN, I-10125 Torino, Italy
⁷⁴Università di Trieste, Dipartimento di Fisica and INFN, I-34127 Trieste, Italy
⁷⁵IFIC, Universitat de Valencia-CSIC, E-46071 Valencia, Spain
⁷⁶University of Victoria, Victoria, British Columbia, Canada V8W 3P6
⁷⁷Department of Physics, University of Warwick, Coventry CV4 7AL, United Kingdom
⁷⁸University of Wisconsin, Madison, Wisconsin 53706, USA

(Dated: October 29, 2018)

We perform a measurement of the CP asymmetry in $b \rightarrow s\gamma$ decays using a sample of 383×10^6 $B\bar{B}$ events collected by the BABAR detector at the PEP-II asymmetric B factory. We reconstruct sixteen flavor-specific B decay modes containing a high-energy photon and a hadronic system X_s containing an s quark. We measure the CP asymmetry to be $-0.011 \pm 0.030(\text{stat}) \pm 0.014(\text{syst})$ for a hadronic system mass between 0.6 and 2.8 GeV/c^2 .

PACS numbers: 13.20.-v, 13.25.Hw

*Deceased

[†]Now at Temple University, Philadelphia, PA 19122, USA

The decay $b \rightarrow s\gamma$ is a flavor-changing neutral current process described by a radiative penguin diagram in the Standard Model (SM). It is sensitive to new physics which can appear in branching fraction or CP asymmetry measurements. Measurements of the branching fraction [1, 2] are in good agreement with the SM [3] predictions.

A CP asymmetry between $b \rightarrow s\gamma$ and $\bar{b} \rightarrow \bar{s}\gamma$ decays is predicted by the SM to be $\leq 1\%$ [4] but could be enhanced up to 15% [5, 6, 7] in models of physics beyond the SM. Existing measurements are consistent with zero CP asymmetry with a precision of 5% [8, 9]. The increased precision obtained in this work allows us to better discriminate between various theoretical models [10].

We use a sample of 383×10^6 $B\bar{B}$ pairs collected at the $\Upsilon(4S)$ resonance by the *BABAR* detector [11] at the PEP-II e^+e^- B factory. In addition, we use 36.3 fb^{-1} collected 40 MeV below the $\Upsilon(4S)$ resonance to study backgrounds from non- B decays.

We reconstruct 16 exclusive $b \rightarrow s\gamma$ final states:

$$\begin{aligned} B^- &\rightarrow K_s^0\pi^-\gamma, K^-\pi^0\gamma, K^-\pi^+\pi^-\gamma, K_s^0\pi^-\pi^0\gamma, \\ &K^-\pi^0\pi^0\gamma, K_s^0\pi^+\pi^-\pi^-\gamma, K^-\pi^+\pi^-\pi^0\gamma, \\ &K_s^0\pi^-\pi^0\pi^0\gamma, K^-\eta\gamma, K^+K^-K^-\gamma, \\ \bar{B}^0 &\rightarrow K^-\pi^+\gamma, K^-\pi^+\pi^0\gamma, K^-\pi^+\pi^-\pi^+\gamma, K^-\pi^+\pi^0\pi^0\gamma, \\ &K^-\pi^+\eta\gamma, K^+K^-K^-\pi^+\gamma, \end{aligned}$$

and measure the yield asymmetry with respect to their charge conjugate decays $\bar{b} \rightarrow \bar{s}\gamma$. These modes are selected because the particles in the final state identify the flavor of the B meson and they can be reconstructed with high statistical significance.

The high-energy photon from the B decay is reconstructed from an isolated energy cluster in the calorimeter, with a shape consistent with the electromagnetic shower produced by a single photon, and an energy $E_\gamma^* > 1.6$ GeV in the $\Upsilon(4S)$ center-of-mass (CM) frame.

The hadronic system X_s , formed from the kaons and pions, is required to have an invariant mass M_{X_s} between 0.6 and 2.8 GeV/c^2 , corresponding to a photon energy threshold $E_\gamma > 1.9$ GeV in the B meson rest frame.

Charged kaons are identified by combining information from the Cherenkov detector and the energy-loss measurements from the tracking system. The remaining tracks are assumed to be charged pions. The K_s^0 candidates are reconstructed by combining two oppositely charged pions with an invariant mass within 9 MeV/c^2 of the nominal K_s^0 mass [12] and a minimum flight distance of 2 mm from the primary event vertex. Both charged

and neutral kaons are required to have laboratory momenta $\geq 0.8\text{ GeV}/c$.

Neutral pions and η candidates are reconstructed from pairs of photons with energies above 50 MeV in the laboratory frame and a lateral moment [13] less than 0.8. The lateral moment measures the spread of a shower in the calorimeter and provides good separation between electromagnetic and hadronic showers. The invariant mass of the pair of photons is required to be between 115 and 150 MeV/c^2 for π^0 candidates and between 470 and 620 MeV/c^2 for η candidates

Monte Carlo (MC) samples based on EvtGen [14] and GEANT4 [15] are used to simulate the signal and background processes and the detector response. The $b \rightarrow s\gamma$ signal sample is generated with a photon spectrum derived from Ref.[4] assuming $m_b = 4.65\text{ GeV}/c^2$. The fragmentation of the X_s system is modeled using JETSET[16] corrected to fit the *BABAR* data as described later.

The background to the B reconstruction is dominated by continuum processes ($e^+e^- \rightarrow q\bar{q}$, with $q = u, d, s, c$) that produce a high-energy photon either by initial-state radiation or from the decay of π^0 and η mesons. Continuum events tend to be less isotropic than B -decay events since they result from hadronic fragmentation of high-momentum quarks back-to-back in the CM frame. High-energy photons in these events tend to be collinear with the thrust axis formed from the rest of the event (ROE), defined as those particles not used in reconstructing the signal B candidate. We reject such backgrounds by requiring that the cosine of the angle between the photon and the thrust axis of the ROE (in the CM frame) be less than 0.85. We further reject the continuum events by requiring the ratio of the second (L_2) and zeroth (L_0) Legendre moments for the ROE particles with respect to the B flight direction to be smaller than 0.46.

Continuum events with high-energy photons from π^0 and η decays are major backgrounds. To veto these events, we associate each high-energy photon candidate γ with another photon candidate γ' in the event. For multiple γ' candidate in an event, we choose the $\gamma\gamma'$ pairs whose invariant mass, determined from adding the four vectors, is closest to the nominal π^0 mass (or η mass in case of η veto). Events are rejected if the photon pairs are consistent with π^0 or η decays based on the output of a boosted decision tree (BDT) [17] constructed from the energy of the less energetic photon γ' and $m_{\gamma\gamma'}$.

We reject the remaining continuum events by constructing an additional BDT that combines information from a number of variables related to the event shape, the kinematic properties of the B meson, and the flavor-tagging [18] properties of the other B meson in the event. Examples of these variables are the Fox-Wolfram moments [19], and the cosine of the B flight direction computed in the CM frame with respect to the beam axis. Optimization of the selection criteria of the π^0 veto, η veto, and event selection BDTs is performed using an iterative method which maximizes the statistical signal

[‡]Now at Tel Aviv University, Tel Aviv, 69978, Israel

[§]Also with Università di Perugia, Dipartimento di Fisica, Perugia, Italy

[¶]Also with Università di Sassari, Sassari, Italy

significance. After the final event selection, we reject 97% of the continuum background while retaining 55% of the signal events.

Fully reconstructed $b \rightarrow s\gamma$ decays are characterized by two kinematic variables: the beam-energy substituted mass $m_{ES} = \sqrt{s/4 - p_B^*{}^2}$, and the energy difference between the B candidate and the beam energy $\Delta E = E_B^* - \sqrt{s}/2$, where E_B^* and p_B^* are the energy and momentum of the B candidate in the e^+e^- CM frame, and \sqrt{s} is the total CM frame energy. Signal events are expected to have a ΔE distribution centered near zero and a m_{ES} distribution centered at the mass of the B meson. For events with multiple B candidates, we select the one with the smallest $|\Delta E|$.

We perform a one-dimensional fit of m_{ES} to the data in the entire M_{X_s} region ($[0.6, 2.8]$ GeV/ c^2) as well as in five different regions of M_{X_s} ($[0.6, 1.1]$, $[1.1, 1.5]$, $[1.5, 2.0]$ and $[2.0, 2.8]$ GeV/ c^2) to study whether the asymmetry has significant mass dependence. Only candidates in the range $|\Delta E| < 0.10$ GeV and $5.22 < m_{ES} < 5.29$ GeV/ c^2 are considered. Probability density functions (PDFs) are constructed for both signal and background in the five M_{X_s} regions. We use the charge of the reconstructed final state (B^-/B^+) or the charge of the kaon (\bar{B}^0/B^0) to define two flavor categories, and perform a simultaneous fit for the flavor asymmetry in each M_{X_s} region.

The signal events are described by a function $f(m_{ES}) = \exp[-(m_{ES} - \mu_0)^2/(2\sigma_{L,R}^2 + \alpha_{L,R}(m_{ES} - \mu_0)^2)]$ where the parameters are determined by an unbinned fit to the signal MC. In the above function, μ_0 is the peak position of the distribution, $\sigma_{L,R}$ are the widths on the left and right of the peak, and $\alpha_{L,R}$ parameterize the tail on the left and right of the peak, respectively.

The background surviving the final selection can be attributed to one of three sources: continuum events, $B\bar{B}$ events other than $b \rightarrow s\gamma$ decays (referred to as generic $B\bar{B}$), and “cross-feed events”, defined as events containing a $b \rightarrow s\gamma$ decay, but in which the true decay was not correctly reconstructed. The shape of the cross-feed and $B\bar{B}$ background is described by a binned PDF, determined from MC with 1 MeV/ c^2 binning.

The continuum background is described by an ARGUS function [20] determined from a fit to the off-resonance data. In this fit, the m_{ES} distribution is shifted to have the same end-point as that of the on-resonance data.

In the maximum-likelihood fit, all parameters are fixed with the exception of the normalizations of the various components as well as μ_0 , which is determined from fitting the data, since the peak position is not well modeled in the MC simulation. The signal, $B\bar{B}$ and cross-feed shapes are constrained by the MC, while the continuum background shape is fixed to that of off-resonance data. The shapes of the distributions are assumed to be the same for B and \bar{B} candidates, with the exception of the $B\bar{B}$ and cross-feed background, which are allowed to vary between B and \bar{B} in order to eliminate the possibility of a false CP asymmetry. In Figure 1 we present the final fits to the m_{ES} distributions for $b \rightarrow s\gamma$ and $\bar{b} \rightarrow \bar{s}\gamma$ events

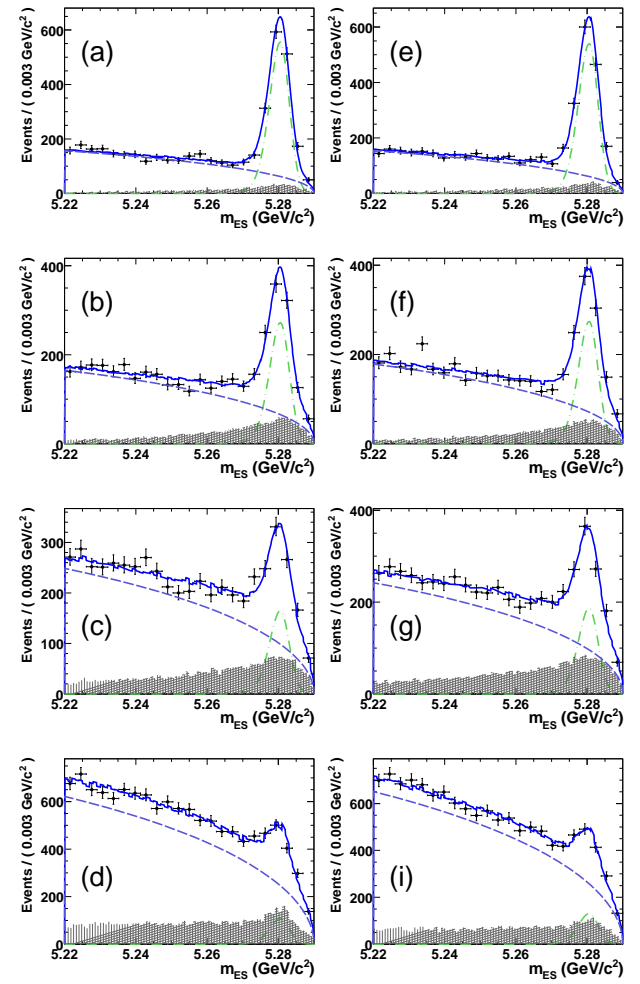


FIG. 1: Fits to the m_{ES} distribution in data for $b \rightarrow s\gamma$ events in M_{X_s} region (a) $[0.6, 1.1]$, (b) $[1.1, 1.5]$, (c) $[1.5, 2.0]$, (d) $[2.0, 2.8]$, and $\bar{b} \rightarrow \bar{s}\gamma$ events in M_{X_s} region (e) $[0.6, 1.1]$, (f) $[1.1, 1.5]$, (g) $[1.5, 2.0]$, (h) $[2.0, 2.8]$. The dashed line shows the shape of the continuum, dotted-dashed line shows the $B\bar{B}$ and cross-feed shape and the dotted line shows the $B\bar{B}$ and cross-feed shape.

for the four M_{X_s} sub-regions. As expected, the signal to background ratio decreases from lower to higher M_{X_s} regions. In Figure 2, we present the final fits to the m_{ES} distribution for $b \rightarrow s\gamma$ and $\bar{b} \rightarrow \bar{s}\gamma$ events for the entire M_{X_s} region.

The direct CP asymmetry is calculated as

$$A_{CP} = \frac{1}{\langle D \rangle} \left(\frac{N_b - N_{\bar{b}}}{N_b + N_{\bar{b}}} - \Delta D \right) - A_{det} \quad (1)$$

where N_b and $N_{\bar{b}}$ are the yields of the $b \rightarrow s\gamma$ and $\bar{b} \rightarrow \bar{s}\gamma$ signals respectively. A_{det} , described in details below, is the flavor bias caused by the detector responses to positively and negatively charged particles. Table I presents the fitted values for $(N_b - N_{\bar{b}})/(N_b + N_{\bar{b}})$.

$\Delta D = (\bar{\omega} - \omega)$ is the difference in the wrong-flavor

M_{X_s} (GeV/c^2)	$\frac{N_b - N_{\bar{b}}}{N_b + N_{\bar{b}}}$	A_{det}	$B\bar{B}$ and cross-feed model syst	Continuum model syst	A_{CP}
0.6–1.1	0.015 ± 0.029	0.005 ± 0.014	0.002	0.004	$0.010 \pm 0.029 \pm 0.015$
1.1–1.5	-0.003 ± 0.049	-0.003 ± 0.015	0.003	0.004	$0.000 \pm 0.049 \pm 0.016$
1.5–2.0	-0.064 ± 0.077	-0.017 ± 0.010	0.010	0.002	$-0.047 \pm 0.077 \pm 0.014$
2.0–2.8	-0.097 ± 0.180	-0.002 ± 0.005	0.070	0.168	$-0.077 \pm 0.180 \pm 0.182$
0.6–2.8	-0.018 ± 0.030	-0.007 ± 0.005	0.012	0.006	$-0.011 \pm 0.030 \pm 0.014$

TABLE I: For each M_{X_s} bin, we present the fitted CP asymmetry: $(N_b - N_{\bar{b}})/(N_b + N_{\bar{b}})$, the flavor-bias of the detector: A_{det} , the systematic error arising from the $B\bar{B}$ and cross-feed modeling and the systematic error arising from the continuum background modeling. The last column shows the final results for the CP asymmetries.

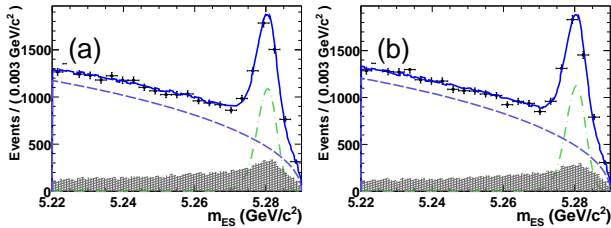


FIG. 2: Fits to the m_{ES} distribution in data for (a) $b \rightarrow s\gamma$ events and (b) $\bar{b} \rightarrow \bar{s}\gamma$ events in the entire M_{X_s} region. The dashed line shows the shape of the continuum, the dotted-dashed line shows the fitted signal shape, and the dotted line shows the $B\bar{B}$ and cross-feed shape.

fraction between b and \bar{b} decays, and $\langle D \rangle = 1 - (\bar{\omega} + \omega)$ is the dilution factor from the average wrong-flavor fraction. The small wrong-flavor fraction $\bar{\omega}$ (ω), defined to be the fraction of \bar{b} (b) reconstructed as the opposite flavor, is due to charged pions misidentified as charged kaons. Using the particle misidentification rate measured in control samples in data we calculate $\Delta D = (5 \pm 4) \times 10^{-5}$ and $1 - \langle D \rangle = (5.4 \pm 0.1) \times 10^{-3}$.

The flavor bias of the detector A_{det} is due to asymmetric K^+, K^- interaction cross-sections in the detector at low momenta. Such an asymmetry could produce a false CP asymmetry in the signal events. We perform a measurement of A_{det} in data using two independent methods. The first approach determines this asymmetry from events in the m_{ES} sideband, $5.22 < m_{ES} < 5.27 \text{ GeV}/c^2$, which is dominated by continuum background with no expected CP asymmetry. The second approach uses a control sample where we replace the high-energy photon from the B decay with a high-energy π^0 with $p_{CM} \geq 1.6 \text{ GeV}/c$. The same selection criteria used in the signal selection are applied, except for π^0 and η veto requirements, and the CP asymmetry in the m_{ES} sideband is measured. In both control samples we apply appropriate weights to the events to ensure that the fraction of each reconstructed final state is identical to that in the signal sample. We find the CP asymmetry measured using both of these approaches to be nearly identical, and average the two measurements to obtain $A_{det} = -0.007 \pm 0.005$. The mean value is used to shift the $(N_b - N_{\bar{b}})/(N_b + N_{\bar{b}})$

mean value, while the error contributes to the systematics. The values of A_{det} computed in each X_s mass region are reported in Table I.

The shape of the $B\bar{B}$ and cross-feed background, determined from MC, is also a potential source of flavor bias in the fit to the data. This background peaks broadly in the signal region, and a small shape difference as a function of flavor could create a false CP asymmetry in the signal. We measure the size of this effect by correcting the $B\bar{B}$ and cross-feed shapes separately. The high-energy π^0 control sample is used to study the uncertainty of the $B\bar{B}$ background shape. We use the differences found between the data and MC m_{ES} shapes in this control sample to correct the nominal $B\bar{B}$ background shape built from the MC. The biggest uncertainty in the cross-feed shape is due to the fact that JETSET does not reproduce the observed fragmentation structure of data. We thus correct the simulation shape using the fragmentation previously determined from *BABAR* data [21]. We then construct new b and \bar{b} binned PDFs using these corrected cross-feed and $B\bar{B}$ events and fit the data a second time with them. The difference between the nominal A_{CP} and A_{CP}' from this fit, shown in Table I, is used as the systematic error from shape modeling of the B background.

The systematic error arising from the continuum background modeling is determined by varying the ARGUS shape parameters within the experimental errors, and is found to be 0.006 for the combined M_{X_s} region. Systematic errors due to possible differences in the signal shape between b and \bar{b} events, CP content of the peaking background, and possible contaminations from $b \rightarrow d\gamma$ decays are all found to be negligible. Contributions from $\langle D \rangle$, ΔD and signal modeling are neglected due to their small impact on A_{CP} . The dominant systematic errors are therefore due to the uncertainties in the flavor bias of the detector and the background shapes as described above.

The total systematic errors are calculated as the sum in quadrature of errors on A_{det} , systematic errors arising from the continuum, $B\bar{B}$ and cross-feed shape modeling. The results are shown in Table I.

In summary, we measure the direct CP asymmetry in $b \rightarrow s\gamma$ to be $A_{CP} = -0.011 \pm 0.030 \pm 0.014$ in the region $0.6 < M_{X_s} < 2.8 \text{ GeV}/c^2$. This result represents the most accurate measurement of this quantity to date. The mea-

surement is consistent with zero CP asymmetry and with the SM prediction. The CP asymmetry in each M_{X_s} region considered in our study is also consistent with zero.

We are grateful for the excellent luminosity and machine conditions provided by our PEP-II colleagues, and for the substantial dedicated effort from the computing organizations that support *BABAR*. The collaborating institutions wish to thank SLAC for its support and

kind hospitality. This work is supported by DOE and NSF (USA), NSERC (Canada), CEA and CNRS-IN2P3 (France), BMBF and DFG (Germany), INFN (Italy), FOM (The Netherlands), NFR (Norway), MES (Russia), MEC (Spain), and STFC (United Kingdom). Individuals have received support from the Marie Curie EIF (European Union) and the A. P. Sloan Foundation.

-
- [1] *BABAR* Collaboration, B. Aubert *et al.*, Phys. Rev. **D72**, 052004 (2005).
 - [2] *BABAR* Collaboration, B. Aubert *et al.*, Phys. Rev. Lett. **97**, 171803 (2006).
 - [3] M. Misaki *et al.*, Phys. Rev. Lett. **98**, 022002 (2007).
 - [4] A. L. Kagan and M. Neubert, Phys. Rev. **D58**, 094012 (1998).
 - [5] L. Wolfenstein and Y. L. Wu, Phys. Rev. Lett. **73**, 2809 (1994).
 - [6] H. M. Asatrian and A. N. Ioannisian, Phys. Rev. **D54**, 5642 (1996).
 - [7] M. Ciuchini, E. Gabrielli, and G. F. Giudice, Phys. Lett. **B388**, 353 (1996).
 - [8] *BABAR* Collaboration, B. Aubert *et al.*, Phys. Rev. Lett. **93**, 021804 (2004).
 - [9] Belle Collaboration, S. Nishida *et al.*, Phys. Rev. Lett. **93**, 031803 (2004).
 - [10] T. Hurth, E. Lunghi, and W. Porod, Nucl. Phys. **B704**, 56 (2005).
 - [11] *BABAR* Collaboration, B. Aubert *et al.*, Nucl. Instrum. Methods **A479**, 1 (2002).
 - [12] W. M. Yao *et al.* (Particle Data Group), J. Phys. **G33**, 1 (2006).
 - [13] A. Drescher *et al.*, Nucl. Instrum. Meth. **A237**, 464 (1985).
 - [14] D. J. Lange, Nucl. Instrum. Meth. **A462**, 152 (2001).
 - [15] GEANT4 Collaboration, S. Agostinelli *et al.*, Nucl. Instrum. Methods **A506**, 250 (2003).
 - [16] T. Sjostrand, Computer Phys. Commun. **82**, 74 (1994).
 - [17] Y. Freund and R. Schapire (????).
 - [18] *BABAR* Collaboration, B. Aubert *et al.*, Phys. Rev. Lett. **89**, 201802 (2002).
 - [19] G. C. Fox and S. Wolfram, Phys. Rev. Lett. **41**, 1581 (1978).
 - [20] ARGUS Collaboration, H. Albrecht *et al.*, Phys. Lett. **B185**, 218 (1987).
 - [21] *BABAR* Collaboration, B. Aubert *et al.*, Phys. Rev. **D72**, 052004 (2005).